

铝合金气体输送活性钨极氩弧焊方法

黄 勇^{1,2}, 李 涛², 王艳磊²

(1. 兰州理工大学 甘肃省有色金属新材料省部共建国家重点实验室, 兰州 730050;

2. 兰州理工大学 有色金属合金及加工教育部重点实验室, 兰州 730050)

摘 要: 针对铝合金 提出了一种气体输送活性钨极氩弧焊, 即 GTFA-TIG 焊(gas transfer flux activating TIG welding). 该方法改变了活性元素的引入方式, 通过自动送粉装置将活性剂输送到保护气体中, 由保护气体将其引入电弧—熔池系统进行施焊, 使得电弧收缩, 熔池金属流态改变, 熔深增加, 同时省却了涂覆活性剂工序, 实现了焊接过程自动化. 进行了普通交流 TIG 焊和 8 种单组元活性剂的 GTFA-TIG 表面熔焊, 分析了不同活性剂对焊缝成形、拉伸性能以及缺陷的影响. 结果表明, 大多数卤化物和氧化物活性剂都能使熔深增加到传统 TIG 焊的 2.5 ~ 3 倍以上, 单质铈增加熔深效果较差. 采用 V_2O_5 的焊缝抗拉强度接近母材金属, 而采用 $MnCl_2$ 和 AlF_3 的焊缝有一定程度降低. 焊缝 X 射线探伤结果表明, 采用 V_2O_5 , $MnCl_2$ 和 AlF_3 的焊缝评片结果均为 I 级, 而采用铈的焊缝为 III 级.

关键词: 气体输送活性钨极氩弧焊; 铝合金; 电弧收缩; 活性剂

中图分类号: TG403 **文献标识码:** A **文章编号:** 0253-360X(2014)01-0101-04

0 序 言

近些年来, 活性焊接法引起了世界范围内的重视^[1,2], 它起初由乌克兰巴顿焊接研究所(PWI)于 20 世纪 60 年代提出, 并引入到钛合金的焊接. 目前针对铝合金已提出的活性焊接方法主要有传统 A-TIG 焊, 法国学者 Sire 等人^[3]开发的 FB-TIG 焊, 以及兰州理工大学开发的 FZ-TIG 焊三种.

传统的 A-TIG 焊是焊前在待焊焊道表面涂覆一层很薄的表面活性剂, 可使熔深显著增加. 然而焊接铝合金时, 很难同时保证熔深显著增加和焊缝表面成形良好^[4]. FB-TIG 焊是将活性剂涂敷于待焊焊道两侧, 中间留出一定间隙, 然后进行常规 TIG 焊, 使得电弧弧根收缩, 熔深增加. FB-TIG 焊虽能保证焊缝表面成形良好, 但熔深增加程度不够理想. FZ-TIG 焊是焊前在待焊焊道表面中心区域涂敷低熔、沸点和低电阻率的活性剂, 在两侧区域分别涂敷高熔、沸点和高电阻率的活性剂, 然后进行常规 TIG 焊, 可同时保证焊接熔深增加和焊缝表面成形良好^[5]. 但是同上述两种方法一样, 该方法仍然需要人工或机械涂敷活性剂, 涂敷厚度不易精确控制, 导致焊接生产效率降低, 焊缝成形不易控制.

针对铝合金, 提出一种新型活性 TIG 焊接方法—气体输送活性钨极氩弧焊, 即 GTFA-TIG 焊(gas

transfer flux activating TIG welding). 该方法改变了活性元素的引入方式, 由自动送粉装置通过保护气体将活性剂输送到焊接电弧—熔池系统中, 从而收缩焊接电弧, 改变熔池金属流态, 增加焊缝熔深.

1 试验方法

试验选用的铝合金为 3A21, 试件尺寸为 150 mm × 80 mm × 8 mm. 分别采用交流 TIG 焊、GTFA-TIG 焊进行表面熔焊, 工艺参数分别如表 1 和表 2 所示. GTFA-TIG 焊的试验装置如图 1 所示, 送粉器为螺旋式送粉器, 通过电机传动能够自动输送定量活性剂. 活性剂采用 $MnCl_2$, AlF_3 , MgF_2 , SiO_2 , Al_2O_3 , N_2O_5 和 TiO_2 等 7 种常见的卤化物和氧化物以及单质铈, 活性剂粒度为 100 目 ~ 200 目.

GTFA-TIG 焊前, 首先加热活性剂, 使活性剂吸附的水分以及本身的结晶水完全脱去, 研磨并筛分. 试样先用丙酮擦拭, 除去表面油污, 然后再将试样用 5% ~ 10% NaOH 溶液清洗 3 ~ 7 min, 使用流动清水冲洗, 再用 30% HNO_3 溶液中和 1 ~ 3 min, 同样用流动清水冲洗, 最后使用吹风机吹干试样. 焊接开始的同时输送活性剂粉末, 熄弧后停止送粉.

采用 8 种单组元活性剂进行交流 GTFA-TIG 焊, 分析不同活性剂对焊缝成形、焊缝拉伸力学性能和焊缝缺陷的影响, 与传统交流 TIG 焊对比研究该新型活性焊接方法的可行性.

表 1 交流 TIG 焊工艺参数
Table 1 Specification of AC TIG welding

焊接电流	焊接速度	弧长	氩气流量	钨极直径	钨极伸出长度
I/A	$v/(mm \cdot min^{-1})$	L/mm	$q/(L \cdot min^{-1})$	d/mm	L_1/mm
130	100	3	10	3.2	3

表 2 交流 GTFA-TIG 焊工艺参数
Table 2 Specification of AC GTFA-TIG welding

焊接电流	焊接速度	弧长	氩气流量	电机转速	钨极直径	钨极伸出长度
I/A	$v/(mm \cdot min^{-1})$	L/mm	$q/(L \cdot min^{-1})$	$n/(r \cdot min^{-1})$	d/mm	L_1/mm
130	100	3	10	30	3.2	3

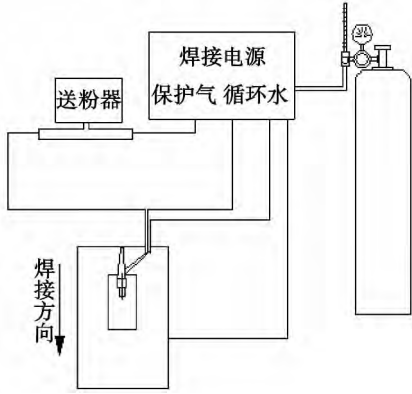


图 1 GTFA-TIG 焊试验装置示意图
Fig. 1 Schematic of GTFA-TIG welding

2 试验结果

2.1 焊缝成形结果

交流 TIG 和 GTFA-TIG 焊的焊缝表面和横截面形貌如图 2 所示,焊缝尺寸如表 3 所示。

试验结果表明,除 MgF_2 和 TiO_2 以外, $MnCl_2$, AlF_3 , SiO_2 , V_2O_5 , Al_2O_3 这 5 种卤化物和氧化物增加熔深的效果都很好,都能使熔深达到传统 TIG 焊熔深的 2.5 ~ 3 倍。其中卤化物活性剂 $MnCl_2$ 和 AlF_3 分别使熔深增加到传统 TIG 焊的 3.0 倍和 2.8 倍,氧化物活性剂 SiO_2 , V_2O_5 和 Al_2O_3 分别使熔深增加到传统 TIG 焊熔深的 3.1 倍、2.8 倍和 2.5 倍,而单质碲增加熔深的效果则相对较差,只使熔深增加到传统 TIG 焊熔深的 1.9 倍。从焊缝表面成形来看,采用 $MnCl_2$ 、碲活性剂的 GTFA-TIG 焊焊缝成形最好, SiO_2 , AlF_3 , Al_2O_3 活性剂的其次,而 V_2O_5 , MgF_2 和 TiO_2 的则较差。

2.2 焊缝拉伸力学性能分析

按国家标准 GB/T228—2002,对母材以及采用 $MnCl_2$, AlF_3 和 V_2O_5 活性剂的 GTFA-TIG 焊缝进行了拉伸试验,试样尺寸如图 3 所示,拉伸速度为 0.5

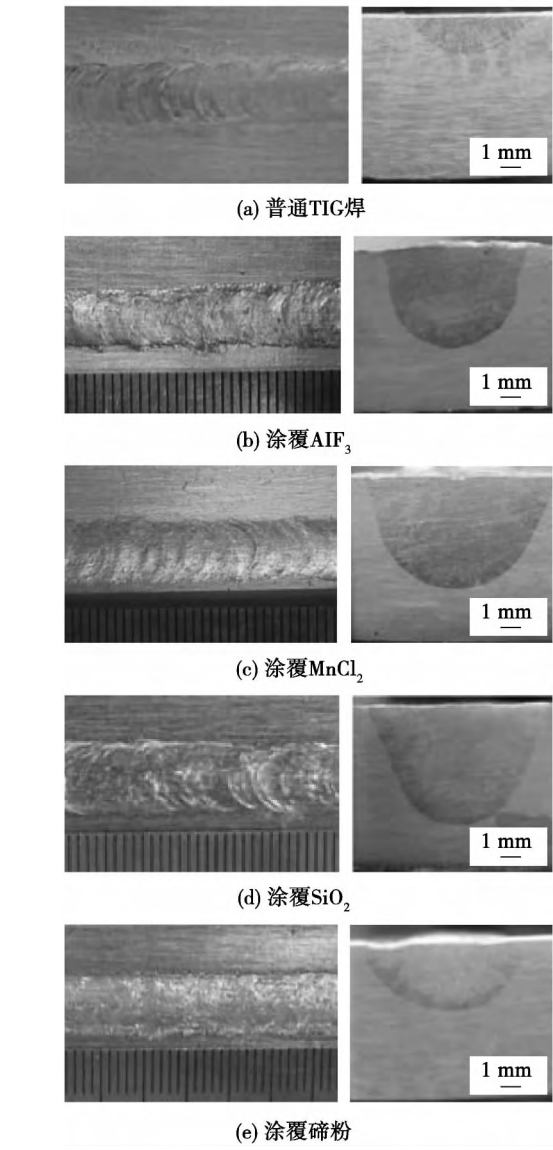


图 2 TIG 焊和 GTFA-TIG 焊的焊缝形貌
Fig. 2 Weld appearances of TIG and GTFA-TIG welding

mm/min。采用碲的 GTFA-TIG 焊缝由于存在气孔,不进行拉伸试验。拉伸结果如表 4 所示。

试验结果表明,采用卤化物 $MnCl_2$ 和 AlF_3 活性

表 3 交流 TIG 和 GTFA-TIG 焊缝尺寸
Table 3 Weld geometry of AC TIG and GTFA-TIG welding

方法	活性剂	熔深 D/mm	熔宽 W/mm	深宽比 n
普通 TIG 焊		1.81	6.02	0.30
GTFA-TIG 焊	AlF_3	5.05	7.29	0.69
	MnCl_2	5.48	8.91	0.62
	MgF_2	2.79	7.38	0.38
	SiO_2	5.62	9.05	0.62
	V_2O_5	5.14	9.77	0.53
	Al_2O_3	5.04	14.25	0.35
	TiO_2	2.93	7.57	0.39
	Te	3.35	8.35	0.40

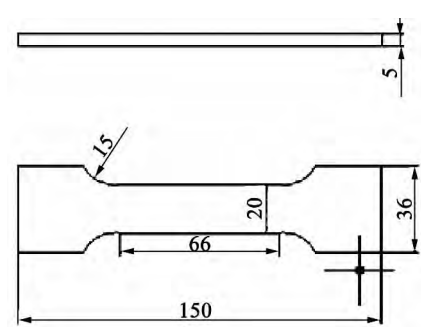


图 3 拉伸试样几何尺寸 (mm)
Fig. 3 Size of tensile sample

表 4 采用不同活性剂的 GTFA-TIG 焊缝抗伸试验结果
Table 4 Tensile test results of GTFA-TIG weld with different activating agent

	活性剂	断后伸长率 $A(\%)$	断面收缩率 $Z(\%)$	抗拉强度 R_m/MPa
GTFA-TIG 焊缝	MnCl_2	0.135	0.615	98.57
	AlF_3	0.115	0.570	93.98
	V_2O_5	0.155	0.730	109.37
母材		0.110	0.650	116.01

剂的 GTFA-TIG 焊试样均断于焊缝区,最大抗拉强度较母材有一定的下降,分别达到母材的 85% 和 81%,而采用氧化物 V_2O_5 活性剂的则均断于焊缝热影响区,最大抗拉强度达到母材的 94%.

2.3 焊缝缺陷分析

选取了四种典型活性剂 MnCl_2 、 AlF_3 、 V_2O_5 和碲粉进行 GTFA-TIG 焊,每种活性剂焊两道焊缝,对所得的 8 条焊缝进行 X 射线探伤. 探伤参数为:管电压 150 kV,管电流 5 mA,曝光时间 4 min. 探伤结果为:除采用碲粉活性剂的焊缝评片结果为Ⅲ级,存在气孔外,采用其它三种活性剂的焊缝评片结果均为Ⅰ级. 说明采用卤化物 MnCl_2 、 AlF_3 和氧化物 V_2O_5

活性剂的 GTFA-TIG 焊缝未发现气孔、夹渣、裂纹和条形缺陷,即采用 GTFA-TIG 焊接方法,可以获得质量良好的焊缝.

3 分析与讨论

在 GTFA-TIG 焊接中, MnCl_2 、 AlF_3 、 SiO_2 、 V_2O_5 、 Al_2O_3 都能使熔深达到传统 TIG 焊熔深的 2.5 ~ 3 倍以上,即使单质碲也能达到 1.9 倍. 而关于活性 TIG 焊熔深增加的作用机理,目前主要有电弧收缩理论和 Marangoni 对流改变两种理论^[6]. 以往的研究表明^[5],对于铝合金,熔深增加的主要机理是电弧收缩,而与 Marangoni 对流变化关系不大,这是由于铝合金表面张力较低,热导率较高,以致材料表面张力温度系数和温度梯度都较低,从而导致 Marangoni 对流较弱,因此,对增加铝合金焊缝熔深的作用不大. 普通交流 TIG 焊和 GTFA-TIG 焊电弧形貌如图 4 所示,试验过程中发现,相同参数下 GTFA-TIG 焊电弧电压比普通 TIG 焊的高 3 ~ 6 V 左右,由此可证明 GTFA-TIG 焊电弧的确发生了强烈收缩. 对于铝合金 GTFA-TIG 焊,电弧收缩应该是熔深增加的主要机理.

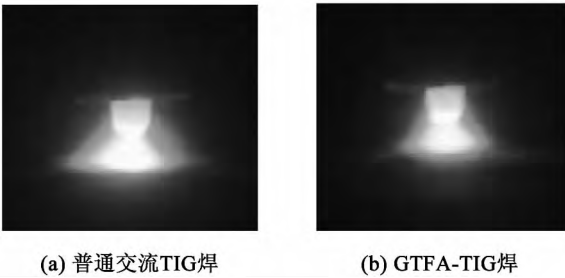


图 4 电弧形貌
Fig. 4 Appearances of welding arc

在电弧外围低温区域,粒子运动速度较慢,活性剂蒸发到电弧中所产生的中性原子和分子易捕捉电子形成负离子,正离子有可能捕捉电子形成低价正离子或者中性原子,导致在作为载流子的电子数量减少,弧柱高温等离子区收缩,电流密度增大,电磁力增加,使熔池内电磁力驱动的向内环流增强,增加熔深. 如表 5 所示,卤化物、氧化物和碲活性剂中的

表 5 元素的电子亲和能 (kJ/mol)
Table 5 Electron affinity energy of element

Ar	O	Cl	F	Te
0	141.0	348.8	327.9	190.4

O、Cl、F 和 Te 元素有较高的电子亲和能,容易捕捉电弧外围电子,使电弧收缩。另外卤化物和氧化物为多原子分子,在电弧作用下发生热解离,而热解离为吸热反应。根据最小电压原理,电弧收缩。几种活

性剂的标准摩尔生成焓如表 6 所示^[7]。电弧在上述两种作用下发生强烈收缩,使得电压增加,热输入增大,同时使电弧和熔池内的电磁力增大,电弧热量更有效传输到熔池底部,焊缝熔深显著增加。

表 6 活性剂标准摩尔生成焓
Table 6 Standard molar formation enthalpy of flux

活性剂	MnCl ₂	AlF ₃	MgF ₂	SiO ₂	V ₂ O ₅	Al ₂ O ₃	TiO ₂
$\Delta H_{f,298}^0 / (\text{kJ} \cdot \text{mol}^{-1})$	-481.997	-1 510.424	-1 123.404	-908.346	-1 557.703	-1 675.700	-944.747

4 结 论

(1) 针对铝合金材料,提出了一种新型活性 TIG 焊接方法—气体输送活性钨极氩弧焊,该方法改变了活性元素的引入方式,通过自动送粉装置将适量的活性剂输送到焊接保护气体中,由保护气体将活性剂引入电弧—熔池系统进行施焊。可同时保证焊缝熔深成倍增加和焊缝表面成形良好,并且省却了涂覆活性剂工序,实现了焊接过程自动化。

(2) 除 MgF₂ 和 TiO₂ 以外, MnCl₂, AlF₃, SiO₂, V₂O₅, Al₂O₃ 这 5 种卤化物和氧化物增加熔深的效果都很好,都能使熔深达到传统 TIG 焊的 2.5 ~ 3 倍,而单质碲增加熔深的效果则相对较差。采用 MnCl₂ 和碲粉的 GTFA-TIG 焊焊缝成形最好, SiO₂, AlF₃ 和 Al₂O₃ 活性剂的其次,而 V₂O₅, MgF₂ 和 TiO₂ 的则较差。

(3) 采用卤化物 MnCl₂ 和 AlF₃ 活性剂的 GT-FA-TIG 焊缝最大抗拉强度分别达到母材的 85% 和 81%,而采用氧化物 V₂O₅ 活性剂的焊缝最大抗拉强度最高,达到母材的 94%。

(4) 采用卤化物 MnCl₂, AlF₃ 和氧化物 V₂O₅ 活性剂的 GTFA-TIG 焊缝经 X 射线探伤未发现气孔、夹渣、裂纹和条形缺陷,而采用碲粉的焊缝则发现气孔。

参考文献:

- [1] 黄 勇,樊 丁,樊清华. 表面活性剂对铝合金直流正接 A-TIG 焊熔深的影响[J]. 焊接学报, 2004, 25(5): 60-62.

- Huang Yong, Fan Ding, Fan Qinghua. Effect of surface activating flux on welding penetration of A-TIG welding with DCSP mode of aluminum alloy [J]. Transactions of the China Welding Institution, 2004, 25(5): 60-62.
- [2] 张京海,鲁晓声,余 巍. 304 不锈钢氩弧焊焊剂的研究[J]. 材料开发与应用, 2000, 15(6): 1-4.
- Zhang Jinghai, Lu Xiaosheng, Yu Wei. Research on GTAW flux used for 304 stainless steel welding [J]. Development and Application of Materials, 2000, 15(6): 1-4.
- [3] Sire S, Marya S. New perspectives in TIG welding of aluminum through flux application FBTIG process [C] // The 7th International Welding Symposium. Kobe, Japan, 2001: 113-118.
- [4] 黄 勇,樊 丁,樊清华. 活性剂增加铝合金交流 A-TIG 焊熔深机理研究[J]. 机械工程学报, 2006, 42(5): 45-49.
- Huang Yong, Fan Ding, Fan Qinghua. Study of mechanism of activating flux increasing weld penetration of AC A-TIG welding for aluminum alloy [J]. Chinese Journal of Mechanical Engineering, 2006, 42(5): 45-49.
- [5] 黄 勇. 铝合金活性 TIG 焊接法及其熔深增加机理的研究 [D]. 兰州: 兰州理工大学, 2007.
- [6] 刘凤尧,林三宝,杨春利,等. 活性化 TIG 焊中活性剂和焊接参数对焊缝深宽比的影响[J]. 焊接学报, 2002, 23(2): 5-8.
- Liu Fengyao, Lin Sanbao, Yang Chunli, et al. Effect of activating fluxes and welding parameters on weld depth to width ratio in A-TIG welding [J]. Transactions of the China Welding Institution, 2002, 23(2): 5-8.
- [7] 黄 勇,樊 丁,林 涛,等. 活性剂对镁合金直流正接 A-TIG 焊熔深的影响[J]. 焊接学报, 2007, 28(10): 21-24.
- Huang Yong, Fan Ding, Lin Tao, et al. Effects of activating fluxes on DCSP A-TIG weld penetration of magnesium alloy [J]. 2007, 28(10): 21-24.

作者简介: 黄 勇,男,1972 年出生,博士,副教授. 主要从事高效焊接技术的研究. 发表论文 40 余篇. Email: hyorhot@lut.cn

neering , South China University of Technology , Guangzhou 510641 , China) . pp 95 – 100

Abstract: The effect of nano-Sb addition on the growth kinetics of intermetallic compound (IMC) in the joints with Sn-3.0Ag-0.5Cu- x Sb ($x=0$, 0.2 , 1.0 , and 2.0%) solder in re-flow process was investigated. Scanning electron microscope (SEM) was used to observe the microstructure evolution of soldered joints , energy dispersive X-ray (EDX) and x-ray diffractometer (XRD) were used to identify the IMC phases. The results show that some nano-Sb particles were dissolved in Sn-rich phase , some participated in the formation of Ag_3Sb , and the rest dissolved in Cu_6Sn_5 IMC layer. The thickness of IMC layer decreased when the nano-Sb was added. Under the isochronal conditions , the thickness of IMC layer in all soldered joints was minimum when the amount of nano-Sb increased to about 1.0% . The growth exponent n and diffusion coefficient D for IMC layer were determined by curve-fitting. The results reveal that the growth exponent n and diffusion coefficient D decreased with the increase of nano-Sb content. When the amount of nano-Sb increased to about 1.0% , the growth exponent n and diffusion coefficient D were 0.326 and $10.31 \times 10^{-10} \text{ cm}^2/\text{s}$, respectively. Based on the phase diagram analysis and adsorption theory , Sb had better affinity to Sn , and it could reduce the activity of Sn by forming SnSb compound , resulting in decreased driving force and surface energy for formation of Cu-Sn IMC. Therefore , the growth rate of Cu_6Sn_5 grains was suppressed and the growth of IMC layer was retarded.

Key words: reflow soldering; nano-Sb dopant; lead free solder; intermetallic compound

Gas transfer flux activating TIG welding process for aluminum alloy HUANG Yong^{1,2} , LI Tao² , WANG Yanlei² (1. State Key Laboratory of Gansu Advanced Non-ferrous Metal Materials , Lanzhou University of Technology , Lanzhou 730050 , China; 2. Key Laboratory of Non-ferrous Metal Alloys , The Ministry of Education , Lanzhou University of Technology , Lanzhou 730050 , China) . pp 101 – 104

Abstract: A new activating TIG welding process , gas transfer flux activating TIG (GTFA-TIG) welding , is proposed for welding aluminum alloy by changing the introduction method of active elements. In this process , a flux is transferred to shielding gas through an automatic powder feeder , and the shielding gas carries the active elements into the welding arc and weld pool. In this way , the welding arc is contracted , and the flow pattern in the weld pool is changed , finally , the weld depth increases. Without coating the flux , the automation of welding process is realized. Compared to the conventional AC TIG welding , the effects of fluxes on the weld shape , tensile property and defects of GTFA-TIG welding with eight kinds of single-component fluxes were investigated. It proves that most of halide and oxide fluxes can improve the weld depth up to 2.5-3.0 times of that of traditional TIG welding , while the effect of Te flux is less effective. The tensile strength of the joint with V_2O_5 flux is close to that of base metal , but it is lower than that of base metal when using $MnCl_2$ and AlF_3 fluxes. The X-ray detection of defects shows that the welds with V_2O_5 , $MnCl_2$ and AlF_3 fluxes are as-

sessed as grade I , while that with Te flux is grade III.

Key words: GTFA-TIG welding; aluminum alloy; arc contraction; activating flux

Microstructure and mechanical properties of welded joint of nanostructured bainite steel with regeneration FANG Kun¹ , HUANG Nan² , YANG Jianguo^{1,3} , SONG Kuijing¹ , FANG Hongyuan¹ (1. State Key Laboratory of Advanced Welding and Joining , Harbin Institute of Technology , Harbin 150001 , China; 2. Armor Force Technique Institute of PLA Teaching and Training Department , Changchun 130117 , China; 3. Institute of Process Equipment and Control Engineering , Zhejiang University of Technology , Hangzhou 310032 , China) . pp 105 – 108

Abstract: Due to the poor weldability of nanostructured bainite steel , a method called welding with regeneration was proposed to obtain a welded joint with the same microstructure as the base metal , so the welded joint could possess the excellent mechanical properties. Regeneration treatment was used after tungsten inert gas (TIG) welding of nanostructured bainite steel. The microstructures of the welded joint were characterized by X-ray diffraction , scanning electron and transmission electron microscopes. The tensile and microhardness tests were carried out to evaluate the mechanical properties. The results show that nanostructured bainite was obtained in the fusion zone and quenched zone with 300 nm and 70 nm thick bainite plates , respectively. The tensile strength of the welded joint was 1 500 MPa , and the microhardness in the fusion zone was 7 000 MPa , which were almost equivalent to those of the base metal.

Key words: nanostructured bainite steel; regeneration; welding; nano-scale plate; strength

Quality assessment for resistance spot welding based on Bayesian image recognition technology ZHANG Hongjie^{1,2} , ZHANG Jianye^{1,2} , SUI Xiuwu^{1,2} (1. School of Mechanical Engineering , Tianjin Polytechnic University , Tianjin 300387 , China; 2. Tianjin Key Laboratory of Modern Mechatronics Equipment Technology , Tianjin Polytechnic University , Tianjin 300387 , China) . pp 109 – 112

Abstract: A method for converting electrode displacement signal to binary image in resistance spot welding process is proposed. Based on image characteristic analysis , fifteen image features are extracted from the binary image of electrode displacement waveform. The principal component analysis is used to remove the cross correlation among image features , and a series of weld specimens with different welding quality are selected to develop a quality classifier. The test results based on Bayesian image recognition technology of minimum risk show that it is feasible and reliable to utilize the binary image of electrode displacement signal to evaluate the weld quality and the image conserves the information of the weld quality. The algorithm for image feature extraction is simple , efficient and easy to use. At the mean time , the Bayesian image recognition technique with small samples can realize the welding quality assessment rapidly and accurately , and the method has a broad application prospect.

Key words: resistance spot welding; quality assessment; Bayesian statistic analysis; image recognition